

See discussions, stats, and author profiles for this publication at: <https://www.researchgate.net/publication/226155373>

High-temperature crystal chemistry of phenakite (Be_2SiO_4) and chrysoberyl (BeAl_2O_4)

ARTICLE in PHYSICS AND CHEMISTRY OF MINERALS · AUGUST 1987

Impact Factor: 1.54 · DOI: 10.1007/BF00628819

CITATIONS

15

READS

28

2 AUTHORS:



Robert M. Hazen

Carnegie Institution for Science

283 PUBLICATIONS 8,698 CITATIONS

SEE PROFILE



L. W. Finger

Carnegie Institution for Science

158 PUBLICATIONS 8,249 CITATIONS

SEE PROFILE

High-Temperature Crystal Chemistry of Phenakite (Be_2SiO_4) and Chrysoberyl (BeAl_2O_4)

Robert M. Hazen and Larry W. Finger

Geophysical Laboratory, Carnegie Institution of Washington, 2801 Upton Street, NW, Washington, DC 20008, USA

Abstract. Thermal expansion and high-temperature crystal structures of phenakite and chrysoberyl have been determined by x-ray methods at several temperatures to 690° C. Phenakite (hexagonal, space group $R\bar{3}$) has slightly anisotropic thermal expansion; average expansions between 25 and 690° C perpendicular and parallel to the c axis are $\alpha_{\perp} = 5.2 \times 10^{-6} \text{ }^{\circ}\text{C}^{-1}$ and $\alpha_{\parallel} = 6.4 \times 10^{-6} \text{ }^{\circ}\text{C}^{-1}$, respectively. The unit cell volume of phenakite over this temperature range is given by the polynomial expression:

$$V = 1102.9(2) + 0.010(2)T + 1.1(3) \times 10^{-5} T^2.$$

Chrysoberyl (orthorhombic, space group $Pbnm$) has nearly isotropic thermal expansion, with maximum expansivity $8.5 \times 10^{-6} \text{ }^{\circ}\text{C}^{-1}$ parallel to the b axis, and minimum expansivity $7.4 \times 10^{-6} \text{ }^{\circ}\text{C}^{-1}$ parallel to a . The c axis expansivity is $8.3 \times 10^{-6} \text{ }^{\circ}\text{C}^{-1}$. Chrysoberyl volume between 25° and 690° C may be represented by:

$$V = 227.1(2) + 0.003(1)T + 4(2) \times 10^{-6} T^2.$$

The thermal expansion of beryllium, aluminum, and silicon cation coordination polyhedra in phenakite and chrysoberyl are similar to values found in previous studies of minerals in the $\text{BeO}-\text{Al}_2\text{O}_3-\text{SiO}_2$ system. High-temperature structure studies of bromellite (BeO), beryl ($\text{Be}_3\text{Al}_2\text{Si}_6\text{O}_{18}$), phenakite and chrysoberyl all have beryllium tetrahedra that display the same near-zero expansion at room temperature, but increasing expansion at higher temperatures.

Introduction

Mineralogists have long attempted to identify systematic mineral behavior to facilitate predictions of structures and physical properties at elevated temperatures and pressures. Experimental examination of suites of chemically-related minerals provides one way to deduce these patterns. The system $\text{BeO}-\text{Al}_2\text{O}_3-\text{SiO}_2-\text{H}_2\text{O}$ (BASH) includes an ideal assortment of large, well-formed, stoichiometric and ordered crystalline phases in a variety of structure types. High-pressure crystal structure studies have been completed for several BASH system minerals, including bromellite (BeO ; Hazen and Finger 1986), phenakite (Be_2SiO_4 ; Kogure and Takeuchi 1986; Hazen and Au 1986), bertrandite ($\text{Be}_4\text{Si}_2\text{O}_7(\text{OH})_2$; Hazen and Au 1986), beryl ($\text{Be}_3\text{Al}_2\text{Si}_6\text{O}_{18}$) and euclase ($\text{BeAlSiO}_4(\text{OH})$; Hazen et al. 1986), and chrysoberyl (BeAl_2O_4 ; Hazen 1986). Thermal

expansion and high-temperature crystal structures have been reported for bromellite (Hazen and Finger 1986) and beryl (Morosin 1972; Brown and Mills 1986). In the present paper we report thermal expansion and high-temperature structures of phenakite and chrysoberyl. A principal objective of this work is to test predictions of the "polyhedral approach", which is based on the assumption that each type of cation coordination polyhedron has properties (thermal expansivity, for example) that are independent of structure (Hazen 1985). Only three types of cation coordination polyhedra – beryllium and silicon tetrahedra and aluminum octahedra – provide the structural building blocks for most of the phases. These beryllium minerals are thus ideally suited for testing polyhedral modeling.

The crystal structure of phenakite (hexagonal: $R\bar{3}$, $Z = 18$), including anisotropic temperature factors, was reported by Zachariasen (1972) and Downs (1983). Silicon and beryllium are tetrahedrally coordinated by oxygen. These tetrahedra are corner-linked to form a continuous framework with 3-, 4- and 6-member rings. The chrysoberyl structure, which was first described by Bragg and Brown (1926) and subsequently refined by Farrell et al. (1963), has the olivine topology (orthorhombic: $Pbnm$, $Z = 4$; with the mineralogical convention for olivines: $b > c > a$). Oxygens in chrysoberyl form a nearly ideal hexagonal close-packed array in which half of the octahedral sites are occupied by Al and one eighth of the tetrahedral sites contain Be.

The principal objectives of this high-temperature research on phenakite and chrysoberyl are (1) to determine temperature-volume equation-of-state parameters and expansion anisotropies by measuring the temperature variation of unit-cell dimensions; (2) to calculate polyhedral thermal expansion from high-temperature structure data in order to compare polyhedral properties in several BASH minerals; and (3) to identify geometrical changes in the phenakite and chrysoberyl structures that result in expansion.

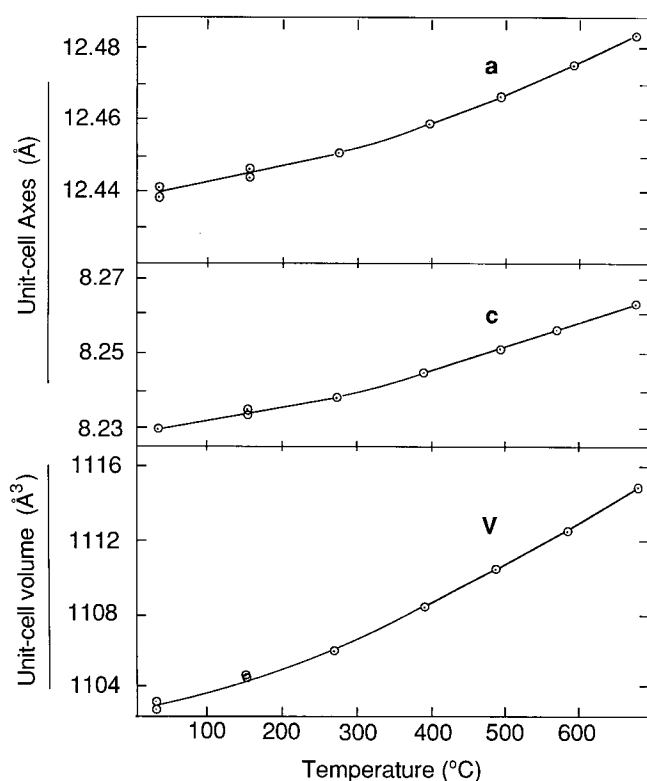
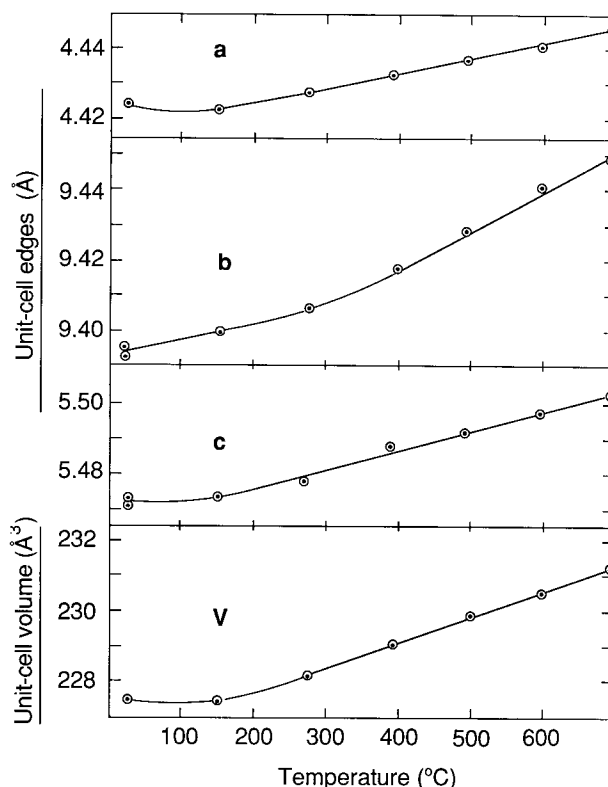
Experimental

Specimen Description

Crystals of natural phenakite from San Miguel di Piracicaba, Brazil (National Museum of Natural History, Smithsonian Institution No. B21152), and natural chrysoberyl

Table 1. Unit cell parameters at several temperatures

Temperature (°C)	<i>a</i> (Å)	<i>c</i> (Å)	<i>V</i> (Å ³)	<i>V/V</i> ₀	<i>c/a</i>
A. Phenakite					
25 before	12.4376 (9) ^a	8.2312 (11)	1102.7 (2)	1.0000	0.6618
25 after	12.4401 (6)	8.2308 (7)	1103.1 (1)	1.0004	0.6616
150 before	12.444 (1)	8.237 (1)	1104.7 (2)	1.0018	0.6619
150 after	12.4464 (6)	8.2361 (7)	1104.9 (1)	1.0020	0.6617
270	12.449 (2)	8.240 (2)	1105.9 (4)	1.0029	0.6619
390	12.4567 (5)	8.2465 (8)	1108.2 (1)	1.0050	0.6620
490	12.4647 (9)	8.2515 (10)	1110.3 (2)	1.0069	0.6620
590	12.473 (2)	8.258 (2)	1112.6 (4)	1.0090	0.6621
690	12.482 (1)	8.266 (1)	1115.2 (3)	1.0113	0.6622
Temperature (°C)	<i>a</i> (Å)	<i>b</i> (Å)	<i>c</i> (Å)	<i>V</i> (Å ³)	<i>V/V</i> ₀
B. Chrysoberyl					
25 before	4.424 (1)	9.396 (1)	5.471 (2)	227.5 (1)	1.0004
25 after	4.424 (1)	9.393 (1)	5.473 (2)	227.4 (1)	1.0000
150	4.4227 (6)	9.3999 (6)	5.4727 (8)	227.52 (5)	1.0005
270	4.4275 (9)	9.4063 (8)	5.477 (1)	228.10 (7)	1.0031
390	4.433 (1)	9.418 (1)	5.488 (2)	229.1 (2)	1.0074
490	4.438 (1)	9.429 (1)	5.492 (2)	229.84 (9)	1.0107
590	4.4407 (6)	9.4409 (5)	5.4970 (7)	230.46 (4)	1.0135
690	4.4457 (5)	9.4491 (5)	5.5011 (6)	231.09 (4)	1.0162

^a Parenthesized figures represent *esd*'s**Fig. 1.** Unit-cell parameters of phenakite as a function of temperature**Fig. 2.** Unit-cell parameters of chrysoberyl as a function of temperature

from Colatina, Espírito Santo, Brazil (National Museum of Natural History, Smithsonian Institution No. R15231) were selected from the same material employed by Barton (1986) in his thermochemical studies of minerals in the BASH system. The phenakite is colorless, transparent and visually free of defects; microprobe analysis revealed no

significant impurities. The chrysoberyl specimen contains 3.1 weight percent Fe_2O_3 , which substitutes for Al_2O_3 , and corresponds to 2.5 mole percent Fe_2BeO_4 .

Room-temperature crystal structures of these phenakite and chrysoberyl specimens have been reported by Hazen and Au (1986) and Hazen (1986), respectively.

Table 2. Refinement conditions and refined atomic parameters of phenakite

		25° C	270° C	490° C	690° C
No. of observations ($I > 2\sigma$)		583	617	504	588
$R(\%)$		4.8	4.0	4.6	4.3
Weighted $R(\%)^b$		3.5	2.9	3.2	3.4
Extinction r^* ($\times 10^5$)		4.0 (3)	3.8 (4)	4.3 (3)	3.7 (3)
Atom	Parameter				
Si	x	0.19553 (7)	0.19557 (5)	0.19546 (1)	0.19554 (6)
	y	0.21167 (7)	0.21152 (5)	0.21158 (6)	0.21162 (6)
	z	0.74982 (9)	0.74995 (6)	0.74992 (9)	0.74998 (8)
	B ^d	0.23 (2)	0.37 (1)	0.52 (2)	0.63 (2)
Be 1	x	0.19403 (36)	0.19384 (25)	0.19445 (35)	0.19381 (33)
	y	0.21011 (36)	0.20985 (26)	0.21063 (32)	0.21010 (34)
	z	0.41557 (36)	0.41545 (28)	0.41563 (40)	0.41550 (36)
	B	0.43 (5)	0.64 (4)	0.88 (5)	1.05 (5)
Be 2	x	0.19456 (37)	0.19430 (25)	0.19380 (34)	0.19426 (32)
	y	0.21201 (35)	0.21157 (25)	0.21103 (32)	0.21133 (33)
	z	0.08466 (37)	0.08379 (28)	0.08446 (41)	0.08448 (37)
	B	0.52 (5)	0.67 (4)	0.86 (5)	1.12 (5)
O 1	x	0.20943 (18)	0.20965 (13)	0.20996 (17)	0.20982 (15)
	y	0.08840 (17)	0.08856 (12)	0.08869 (16)	0.08888 (17)
	z	0.75061 (21)	0.75032 (16)	0.75036 (21)	0.75048 (20)
	B	0.42 (3)	0.59 (2)	0.80 (3)	0.97 (3)
O 2	x	0.33352 (18)	0.33348 (13)	0.33341 (16)	0.33312 (15)
	y	0.33293 (17)	0.33323 (12)	0.33297 (16)	0.33288 (16)
	z	0.74989 (22)	0.75008 (17)	0.74979 (25)	0.75013 (22)
	B	0.36 (3)	0.53 (2)	0.72 (3)	0.93 (3)
O 3	x	0.12217 (18)	0.12234 (13)	0.12248 (17)	0.12248 (16)
	y	0.20972 (17)	0.20978 (13)	0.20986 (16)	0.20976 (17)
	z	0.91520 (22)	0.91468 (17)	0.91459 (22)	0.91413 (21)
	B	0.37 (3)	0.60 (2)	0.78 (3)	0.98 (3)
O 4	x	0.12242 (18)	0.12233 (13)	0.12233 (17)	0.12219 (17)
	y	0.20928 (18)	0.20884 (13)	0.20871 (17)	0.20875 (17)
	z	0.58542 (21)	0.58555 (16)	0.58547 (21)	0.58607 (20)
	B	0.40 (3)	0.57 (2)	0.78 (3)	1.00 (3)

^a Parenthesized figures represent esd 's^b $R = \sum [F_o - F_c] / \sum F_o$ ^c Weighted $R = [\sum w(F_o - F_c)^2 / \sum w F_o^2]^{1/2}$ ^d Equivalent isotropic temperature factors

Data Collection at High Temperature

Equant crystals, approximately 100- μm maximum dimension, were mounted in silica glass capillaries as described by Hazen and Finger (1982). Preliminary, room-temperature studies of each crystal were performed with the heater mounted in the same configuration used in high-temperature experiments. A platinum-wire resistance heater of the type designed by Ohashi (Hazen and Finger 1982) was employed in the measurement of unit-cell parameters and x-ray intensity data on the four-circle diffractometer. Temperature was controlled and corrected for χ axis "chimney effects" by an automated feedback system (Finger et al. 1973). The furnace temperature was calibrated against the known temperature-volume equation-of-state of BeO and CaF₂.

Lattice constants of the two beryllium aluminosilicates were determined at several temperatures. From 12 to 20 reflections were measured by the method of Hamilton (1974), as modified by King and Finger (1979), in order to correct

for errors in crystal centering on the diffractometer as well as diffractometer alignment. Each set of angular data was refined initially without constraint, and the resultant "triclinic" cell was examined for conformity with expected hexagonal and orthorhombic symmetries of phenakite and chrysoberyl, respectively. These symmetry conditions were met within two standard deviations at all temperatures studied. Phenakite and chrysoberyl cell parameters were then refined with hexagonal and orthorhombic constraints, respectively. These high-temperature unit-cell parameters are recorded in Table 1 and are illustrated in Figures 1 and 2.

Intensity data for three-dimensional structure refinements were collected on all reflections accessible within a quadrant with $(\sin \theta)/\lambda \leq 0.7$. Omega increments of 0.025° and counting times of 3 seconds per increment were used. Corrections were made for Lorentz and polarization effects, as well as crystal absorption. Conditions of high-temperature refinements, refined isotropic extinction coefficients (Zachariasen 1967), atomic positional parameters and iso-

Table 3. Refinement conditions and refined parameters of chrysoberyl at several temperatures

		25° C	270° C	490° C	690° C
Number of observations ($I>2\delta$)		308	304	290	300
$R^b(\%)$		2.8	2.3	4.1	2.3
Weighted $R^c(\%)$		4.4	2.3	4.0	2.4
Extinction, r^* ($\times 10^5$)		6.0 (4) ^a	6.0 (3)	4.7 (4)	5.4 (3)
Atom	Parameter				
Al1	x	0	0	0	0
	y	0	0	0	0
	z	0	0	0	0
	B ^d	0.32 (2)	0.46 (2)	0.54 (3)	0.77 (2)
Al2	x	0.9949 (2)	0.9950 (1)	0.9950 (2)	0.9952 (1)
	y	0.27306 (8)	0.27323 (5)	0.27332 (9)	0.27367 (5)
	z	0.25	0.25	0.25	0.25
	B	0.20 (2)	0.33 (2)	0.43 (3)	0.66 (2)
Be	x	0.4333 (7)	0.4340 (5)	0.4353 (9)	0.4357 (5)
	y	0.0929 (4)	0.0925 (3)	0.0929 (5)	0.0930 (3)
	z	0.25	0.25	0.25	0.25
	B	0.44 (4)	0.61 (4)	0.84 (7)	1.03 (4)
O1	x	0.7874 (4)	0.7880 (3)	0.7883 (5)	0.7885 (3)
	y	0.0901 (2)	0.0900 (1)	0.0904 (2)	0.0903 (1)
	z	0.25	0.25	0.25	0.25
	B	0.35 (2)	0.46 (2)	0.57 (4)	0.75 (2)
O2	x	0.2422 (4)	0.2423 (3)	0.2424 (5)	0.2429 (3)
	y	0.4330 (2)	0.4334 (1)	0.4330 (2)	0.4328 (1)
	z	0.25	0.25	0.25	0.25
	B	0.36 (2)	0.49 (2)	0.59 (4)	0.83 (2)
O3	x	0.2568 (3)	0.2570 (2)	0.2576 (4)	0.2579 (2)
	y	0.1631 (1)	0.1632 (1)	0.1628 (2)	0.1627 (1)
	z	0.0154 (2)	0.0154 (1)	0.0156 (3)	0.0154 (2)
	B	0.38 (2)	0.52 (2)	0.61 (3)	0.86 (2)

^a Parenthesized figures represent esd 's^b $R = \sum [F_o - F_c] / \sum F_o$ ^c Weighted $R = [\sum w(F_o - F_c)^2 / \sum w F_o^2]^{1/2}$ ^d Equivalent isotopic temperature factors

tropic thermal parameters are recorded in Tables 2 and 3. Anisotropic thermal parameters, magnitudes and orientations of thermal vibration ellipsoids, and observed and calculated structure factors at 25°, 270°, 490° and 690° C for both phenakite and chrysoberyl are recorded in unpublished tables that are available from the authors on request.

Results

Thermal Expansion

Phenakite and chrysoberyl unit-cell parameters at several temperatures (Table 1; Figures 1 and 2) were used to calculate linear thermal expansivity and temperature-volume equation-of-state parameters. Unit-cell edges were described with a second-order polynomial expression:

For phenakite:

$$a = 12.439 \pm 0.001 + 2.8(\pm 0.8) \times 10^{-5}T + 5(\pm 1) \times 10^{-8}T^2$$

$$c = 8.2306 \pm 0.0005 + 3.0(\pm 0.4) \times 10^{-5}T$$

$$+ 3.0(\pm 0.6) \times 10^{-8}T^2$$

For chrysoberyl:

$$a = 4.422 \pm 0.001 + 1.1(\pm 11) \times 10^{-5}T + 3(\pm 1) \times 10^{-8}T^2$$

$$b = 9.392 \pm 0.002 + 4.6(\pm 15) \times 10^{-5}T + 6(\pm 2) \times 10^{-8}T^2$$

$$c = 5.468 \pm 0.002 + 3(\pm 2) \times 10^{-5}T + 2(\pm 2) \times 10^{-8}T^2.$$

Average phenakite axial thermal expansion over the temperature range 25° to 690° C are $5.2 \times 10^{-6} \text{ }^\circ\text{C}^{-1}$ perpendicular to c and $6.4 \times 10^{-6} \text{ }^\circ\text{C}^{-1}$ parallel to c . Phenakite thermal expansion is thus slightly anisotropic, with the c axis approximately 20% more expansible than a , and a corresponding small increase in c/a with increasing temperature (Table 1).

Orthorhombic chrysoberyl is characterized by nearly isotropic expansion. Average coefficients for expansion parallel to a , b and c are 7.4, 8.5, and 8.3 (all $\times 10^{-6} \text{ }^\circ\text{C}^{-1}$), respectively.

High-Temperature Crystal Structure of Phenakite

Three symmetrically-distinct cation tetrahedra, one Si and two Be, link to form the phenakite framework. The average Si—O distance (Table 4) is constant at $1.627 \pm 0.001 \text{ \AA}$ over the temperature range 25° to 690° C. The volume of the silicon tetrahedron (Table 5) is also unchanged at approximately 2.205 \AA^3 . This polyhedron is close to regular with O—Si—O angles deviating by less than 4° from the ideal 109.5° value.

Both symmetrically-distinct beryllium tetrahedra, on the other hand, expand significantly over the 25° to 690° C

Table 4. Selected bond distances and angles for phenakite

Bond/Angle	25° C	270° C	490° C	690° C
Si Tetrahedron				
Si—O1	1.627 (2) ^a	1.625 (1)	1.630 (2)	1.629 (2)
Si—O2	1.622 (2)	1.625 (1)	1.626 (2)	1.625 (2)
Si—O3	1.633 (2)	1.629 (2)	1.629 (2)	1.628 (2)
Si—O4	1.622 (2)	1.624 (1)	1.625 (2)	1.626 (2)
Mean Si—O	1.626	1.626	1.628	1.627
O1—Si—O2	108.3 (1)	108.5 (1)	108.2 (1)	108.3 (1)
O1—Si—O3	107.7 (1)	108.0 (1)	108.1 (1)	108.0 (1)
O1—Si—O4	108.0 (1)	107.8 (1)	107.8 (1)	107.9 (1)
O2—Si—O3	109.7 (1)	109.6 (1)	109.7 (1)	109.6 (1)
O2—Si—O4	109.9 (1)	109.9 (1)	109.9 (1)	110.0 (1)
O3—Si—O4	113.0 (1)	113.0 (1)	113.1 (1)	112.9 (1)
Be1 Tetrahedron				
Be1—O1	1.639 (4)	1.638 (3)	1.643 (4)	1.645 (4)
Be1—O2	1.637 (4)	1.643 (3)	1.636 (4)	1.649 (4)
Be1—O4	1.636 (4)	1.637 (3)	1.645 (4)	1.643 (4)
Be1—O4	1.655 (4)	1.657 (3)	1.659 (4)	1.665 (4)
Mean Be1—O	1.642	1.644	1.646	1.650
O1—Be1—O2	109.3 (2)	109.3 (2)	109.4 (2)	109.3 (2)
O1—Be1—O4	108.3 (2)	108.5 (2)	108.2 (2)	108.3 (2)
O1—Be1—O4	114.2 (2)	114.3 (2)	114.1 (2)	114.4 (2)
O2—Be1—O4	108.3 (2)	108.3 (2)	108.7 (2)	108.3 (2)
O2—Be1—O4	108.3 (2)	108.3 (2)	108.6 (2)	108.4 (2)
O4—Be1—O4	108.2 (2)	108.1 (2)	107.7 (2)	108.0 (2)
Be2 Tetrahedron				
Be2—O1	1.627 (4)	1.637 (3)	1.632 (4)	1.638 (4)
Be2—O2	1.634 (4)	1.636 (3)	1.647 (4)	1.644 (4)
Be2—O3	1.650 (4)	1.650 (3)	1.650 (4)	1.654 (4)
Be2—O3	1.652 (4)	1.651 (3)	1.656 (4)	1.664 (4)
Mean Be2—O	1.641	1.643	1.646	1.650
O1—Be2—O2	110.4 (2)	109.8 (2)	109.8 (2)	110.0 (2)
O1—Be2—O3	107.9 (2)	107.8 (2)	108.3 (2)	108.0 (2)
O1—Be2—O3	114.0 (2)	114.2 (2)	114.5 (2)	114.2 (2)
O2—Be2—O3	107.8 (2)	107.7 (2)	107.5 (2)	107.7 (2)
O2—Be2—O3	109.0 (2)	109.1 (2)	108.5 (2)	108.7 (2)
O3—Be2—O3	107.5 (2)	108.1 (2)	108.1 (2)	108.0 (2)
O1 (3—coordinated)				
O1—Si	1.627 (2)	1.625 (1)	1.630 (2)	1.629 (2)
O1—Be1	1.639 (4)	1.638 (3)	1.643 (4)	1.645 (4)
O1—Be2	1.627 (4)	1.637 (3)	1.632 (4)	1.638 (4)
Si—O1—Be1	123.1 (2)	123.3 (1)	123.3 (2)	123.2 (2)
Si—O1—Be2	123.7 (2)	123.4 (1)	123.4 (2)	123.6 (2)
Be1—O1—Be2	113.0 (2)	113.1 (1)	113.1 (2)	112.9 (2)
O2 (3—coordinated)				
O2—Si	1.622 (2)	1.625 (1)	1.626 (2)	1.625 (2)
O2—Be1	1.637 (4)	1.643 (3)	1.636 (4)	1.649 (4)
O2—Be2	1.634 (4)	1.636 (3)	1.647 (4)	1.644 (4)
Si—O2—Be1	120.5 (2)	120.2 (1)	120.3 (2)	120.3 (2)
Si—O2—Be2	120.2 (2)	120.3 (1)	120.1 (2)	120.3 (2)
Be1—O2—Be2	119.4 (2)	119.5 (2)	119.5 (1)	119.4 (2)
O3 (3—coordinated)				
O3—Si	1.633 (2)	1.629 (2)	1.629 (2)	1.628 (2)
O3—Be1	1.650 (4)	1.650 (3)	1.650 (4)	1.654 (4)
O3—Be2	1.652 (4)	1.651 (3)	1.656 (4)	1.664 (4)
Si—O3—Be2	114.1 (2)	114.0 (1)	114.3 (2)	114.2 (2)
Si—O3—Be2	123.4 (2)	123.9 (1)	123.6 (2)	123.9 (2)
Be2—O3—Be2	118.3 (1)	121.9 (1)	121.8 (2)	121.7 (2)

Table 4. (continued)

Bond/Angle	25° C	270° C	490° C	690° C
O4 (3—coordinated)				
O4—Si	1.622 (2)	1.624 (1)	1.625 (2)	1.626 (2)
O4—Be1	1.636 (4)	1.637 (3)	1.645 (4)	1.643 (4)
O4—Be1	1.655 (4)	1.657 (3)	1.659 (4)	1.665 (4)
Si—O4—Be1	114.2 (2)	114.3 (1)	114.3 (2)	114.3 (2)
Si—O4—Be1	123.7 (2)	123.7 (1)	123.6 (2)	123.9 (2)
Be1—O4—Be1	118.3 (1)	121.8 (1)	121.9 (2)	121.6 (2)

^a Parenthesized figures represent *esd*'s

temperature interval (Fig. 3). The average Be—O expansion is about $8 \times 10^{-6} \text{ }^\circ\text{C}^{-1}$. Note, however, that this expansion is not uniform over the temperature interval studied. The bond lengths are virtually unchanged between 25° and 270° and expand only slightly to 490°. The most significant variations are seen at higher temperatures, between 490° and 690° C. Beryllium tetrahedra are almost regular, with O—Si—O angles between 107° and 114°. Polyhedral distortions do not change with temperature (Table 5).

The four symmetrically-distinct oxygen atoms are all three-coordinated to one silicon and two berylliums, with the oxygens lying close to the planes defined by the three adjacent cations. Cation-oxygen-cation angles range from 113° to 124°, compared to the ideal 120° value of regular trigonal coordination. None of these Be—O—Be or Be—O—Si angles changes significantly with temperature.

In summary, the only significant phenakite structural variation with temperature is expansion of Be—O bonds. Beryllium tetrahedral expansion is reflected in the bulk thermal expansion of the mineral.

High-Temperature Crystal Structure of Chrysoberyl

All three chrysoberyl cation polyhedra — two aluminum octahedra and a beryllium tetrahedron — display significant expansion. Both Al1—O and Al2—O average bond lengths (Table 6) increase by about 0.01 Å between 25° and 690° C. The average Al—O thermal expansion coefficient is thus about $8 \times 10^{-6} \text{ }^\circ\text{C}^{-1}$. This coefficient also obtains for individual Al1—O bonds; the Al1 octahedron expands relatively uniformly and distortions (Table 5) of the Al1 octahedron (point symmetry $\bar{1}$) are unchanged with temperature. O—Al1—O angles deviate by no more than 8° from the ideal 90° value, and none of the angles varies significantly with temperature.

Individual Al2—O bonds, however, display a much wider range of expansion. The Al2—O2 bond, which lies in the *a*—*b* plane about 35° from *b*, expands by only about $3 \times 10^{-6} \text{ }^\circ\text{C}^{-1}$, whereas two of the Al2—O3 bonds expand by four times this value. The Al2 octahedron (point symmetry *m*) thus becomes more distorted at higher temperatures; O—Al2—O angles deviate from 90° by as much as 11° at room temperature, and these deviations increase with temperature.

The average Be—O bond length of the beryllium tetrahedron (point symmetry *m*) increases from 1.634 Å at 25° C to 1.644 Å at 690° C. The average expansion coefficient over this range is thus about $9 \times 10^{-6} \text{ }^\circ\text{C}^{-1}$. Expansions of individual Be—O bonds display great variation. The Be—O1 bond, which is subparallel to *a* (the least compress-

Table 5. Polyhedral volumes and distortion parameters of phenakite and chrysoberyl at several temperatures

Atom	Parameter	25° C	270° C	490° C	690° C
<i>A. Phenakite</i>					
Si	Vol (Å ³)	2.204 (4) ^a	2.203 (3)	2.209 (4)	2.207 (4)
	QE ^b	1.001 (2)	1.001 (2)	1.001 (2)	1.001 (2)
	AV ^c	4.1	3.8	4.2	3.8
Be 1	Vol (Å ³)	2.267 (7)	2.275 (5)	2.282 (7)	2.302 (7)
	QE	1.002 (4)	1.002 (3)	1.001 (4)	1.002 (4)
	AV	5.8	5.9	5.8	6.2
Be 2	Vol (Å ³)	2.263 (7)	2.272 (5)	2.288 (6)	2.299 (6)
	QE	1.002 (3)	1.002 (2)	1.002 (3)	1.002 (3)
	AV	6.3	6.4	7.0	6.3
<i>B. Chrysoberyl</i>					
Al1	Vol (Å ³)	8.827 (7)	8.844 (5)	8.917 (10)	8.959 (5)
	QE	1.0100 (2)	1.0102 (2)	1.0102 (2)	1.0101 (2)
	AV	36.8	37.3	37.4	37.0
Al2	Vol (Å ³)	9.500 (8)	9.527 (5)	9.594 (10)	9.746 (6)
	QE	1.0142 (11)	1.0144 (7)	1.0147 (13)	1.0147 (7)
	AV	47.0	47.6	48.3	49.3
Be	Vol (Å ³)	2.168 (11)	2.176 (8)	2.190 (13)	2.205 (9)
	QE	1.023 (3)	1.023 (2)	1.024 (3)	1.024 (2)
	AV	104.9	107.7	111.4	112.4

^a Parenthesized figures represent *esd*'s^b QE = Quadratic elongation = $\sum_{i=1}^n [(l_i/l_o)^2/n - 1]$ (Robinson et al. 1971)^c AV = Angle variance = $\sum_{i=1}^n [(\theta_i - \theta_o)^2/n - 1]$ (Robinson et al. 1971)

ible axis), is unchanged within experimental error. In contrast the Be—O2 bond, which is in the *a-b* plane about 30° from *b* (the most expansible axis), has an average expansion of about $20 \times 10^{-6} \text{ }^\circ\text{C}^{-1}$. The beryllium tetrahedron is relatively distorted, with O—Be—O angles ranging from 98.0° to 118.8° at room temperature. This range increases at higher temperatures (97.5° to 119.0° at 690° C).

Three symmetrically-distinct oxygen atoms in chrysoberyl are all four-coordinated to one beryllium and three aluminum cations. No significant changes are observed for any Al—O—Al or Al—O—Be angle.

Discussion

Polyhedral Thermal Expansivities

Hazen and Prewitt (1977) and Hazen and Finger (1982) demonstrated an inverse relationship between average thermal expansion of cation-oxygen bonds in a polyhedron and the Pauling bond strength. They proposed a relationship:

$$\alpha = 32.9 (0.75 - z/p) \times 10^{-6} \text{ }^\circ\text{C}^{-1} \quad (z/p \leq 0.75);$$

$$\alpha = 0 \quad (z/p > 0.75)$$

where α is the mean thermal expansion between 25° and 1000° C, *z* is the cation formal charge and *p* is coordination number. The bond strength, *z/p*, of Si—O tetrahedral bonds is 1, so they are not predicted to expand. The bond strengths of both Be—O tetrahedral bonds and Al—O octahedral

bonds is 0.5, so the predicted average expansion of these bonds in phenakite and chrysoberyl is about $8 \times 10^{-6} \text{ }^\circ\text{C}^{-1}$.

Observed average thermal expansivity for Be—O and Si—O bonds in phenakite (25° to 690° C) are 8 and $0 \times 10^{-6} \text{ }^\circ\text{C}^{-1}$, respectively. Those for Be—O and Al—O bonds in chrysoberyl are 9 and $8 \times 10^{-6} \text{ }^\circ\text{C}^{-1}$, respectively. The observed bond expansivities are thus in excellent agreement with the polyhedral systematics.

Comparison of Beryllium Minerals at High Temperature

Figure 3 illustrates the temperature variation of BeO₄ polyhedral volume for tetrahedra in phenakite, chrysoberyl, bromellite and beryl. It is remarkable that each of the five different tetrahedra can be represented by the same curve, especially considering the differences in the detailed behavior of these polyhedra. In bromellite (Hazen and Finger 1986) and beryl (Brown and Mills 1986), for example, all four individual Be—O bonds have similar expansion coefficients, but in phenakite and chrysoberyl a significant range of bond expansivities is observed. The tetrahedron in beryl is extremely distorted, whereas the bromellite tetrahedron is close to regular. Furthermore, the average room-temperature bond lengths in these compounds range from 1.634 Å in chrysoberyl to 1.675 Å in beryl, presumably because of the differences in second-nearest neighbor topologies.

Important differences also occur in oxygen nearest-neighbor coordination by cations. In bromellite each oxygen is tetrahedrally coordinated by Be; in phenakite the

Table 6. Selected bond distances and angles for Chrysoberyl

Bond/Angle		25° C	270° C	490° C	690° C
Al1—O1	[2]	1.8629 (9)	1.8633 (8)	1.865 (2)	1.8717 (9)
Al1—O2	[2]	1.888 (9)	1.8893 (9)	1.890 (2)	1.8976 (9)
Al1—O3	[2]	1.9093 (9)	1.9123 (9)	1.912 (2)	1.920 (1)
Mean Al1—O		1.887	1.888	1.889	1.896
O1—Al1—O2	[2]	85.61 (4)	85.54 (4)	85.61 (7)	85.56 (4)
O1—Al1—O3	[2]	94.39 (4)	94.46 (4)	94.39 (7)	94.44 (4)
O1—Al1—O3	[2]	84.49 (5)	84.43 (5)	84.36 (8)	84.40 (5)
O1—Al1—O3	[2]	85.51 (5)	95.57 (5)	95.64 (8)	95.60 (5)
O2—Al1—O3	[2]	82.83 (5)	82.82 (4)	82.81 (8)	82.88 (5)
O2—Al1—O3	[2]	97.17 (5)	97.18 (4)	97.19 (8)	97.12 (5)
Al2—O1		1.949 (1)	1.952 (1)	1.949 (2)	1.961 (1)
Al2—O2		1.860 (1)	1.862 (1)	1.859 (2)	1.864 (1)
Al2—O3	[2]	1.8915 (9)	1.8925 (9)	1.893 (2)	1.8991 (9)
Al2—O3	[2]	2.015 (1)	2.0171 (9)	2.020 (2)	2.032 (1)
Mean Al2—O		1.937	1.939	1.939	1.948
O1—Al2—O3	[2]	79.54 (4)	79.44 (4)	79.40 (7)	79.25 (4)
O1—Al2—O3	[2]	91.01 (4)	91.02 (4)	91.12 (7)	91.10 (4)
O2—Al2—O3	[2]	94.08 (4)	94.11 (4)	94.06 (7)	94.18 (4)
O2—Al2—O3	[2]	94.37 (4)	94.42 (4)	94.38 (8)	94.41 (4)
O2—Al2—O3	[2]	89.62 (3)	89.61 (3)	89.68 (4)	89.67 (3)
O3—Al2—O3		79.18 (5)	79.14 (5)	78.91 (9)	78.86 (5)
O3—Al2—O3		100.33 (6)	100.36 (6)	100.48 (10)	100.51 (6)
Be—O1		1.568 (2)	1.567 (2)	1.563 (5)	1.569 (3)
Be—O2		1.687 (3)	1.688 (3)	1.698 (5)	1.709 (3)
Be—O3	[2]	1.641 (2)	1.645 (2)	1.643 (3)	1.650 (2)
Mean Be—O		1.634	1.636	1.637	1.644
O1—Be—O2		116.4 (2)	116.7 (2)	116.7 (3)	116.7 (2)
O1—Be—O3	[2]	118.8 (1)	118.9 (1)	119.0 (2)	119.0 (1)
O2—Be—O3	[2]	98.0 (1)	97.9 (1)	97.6 (2)	97.5 (1)
O3—Be—O3		102.9 (2)	102.7 (2)	102.8 (3)	102.9 (2)
O1—Be		1.568 (2)	1.567 (2)	1.563 (5)	1.569 (3)
O1—Al1	[2]	1.8629 (9)	1.8633 (8)	1.865 (2)	1.8717 (9)
O1—Al2		1.949 (1)	1.952 (1)	1.949 (2)	1.961 (1)
Be—O1—Al1	[2]	120.79 (7)	120.70 (7)	120.6 (1)	120.6 (1)
Be—O1—Al2		117.2 (1)	117.1 (1)	117.1 (2)	117.0 (1)
Al1—O1—Al1		94.52 (6)	94.59 (6)	94.5 (1)	94.57 (6)
Al1—O1—Al2	[2]	99.37 (5)	99.47 (5)	99.6 (1)	99.63 (5)
O2—Be		1.687 (3)	1.688 (3)	1.698 (5)	1.709 (3)
O2—Al1	[2]	1.8888 (9)	1.8893 (9)	1.890 (2)	1.8976 (9)
O2—Al1		1.860 (1)	1.862 (1)	1.859 (2)	1.864 (1)
Be—O2—Al1	[2]	89.00 (7)	89.15 (7)	89.1 (1)	89.06 (8)
Be—O2—Al2		116.6 (1)	116.4 (1)	116.3 (2)	116.1 (1)
Al1—O2—Al1		92.84 (6)	92.90 (6)	92.8 (1)	92.90 (6)
Al1—O2—Al2	[2]	128.61 (4)	128.56 (4)	128.69 (7)	128.73 (4)
O3—Be		1.641 (2)	1.645 (2)	1.643 (3)	1.650 (2)
O3—Al1		1.9093 (9)	1.9123 (9)	1.912 (2)	1.920 (1)
O3—Al2		1.8915 (9)	1.8925 (9)	1.893 (2)	1.8991 (9)
O3—Al2		2.015 (1)	2.0171 (9)	2.020 (2)	2.032 (1)
Be—O3—Al1		89.65 (9)	89.64 (9)	90.0 (2)	90.04 (10)
Be—O3—Al2		88.93 (8)	89.08 (8)	89.1 (1)	89.12 (8)
Be—O3—Al2		117.65 (9)	117.53 (9)	117.5 (2)	117.48 (9)
Al1—O3—Al2		95.57 (4)	95.62 (4)	95.58 (7)	95.63 (4)
Al1—O3—Al2		123.48 (5)	123.45 (5)	123.45 (8)	123.45 (5)
Al2—O3—Al2		130.32 (5)	130.33 (5)	130.2 (1)	130.13 (5)

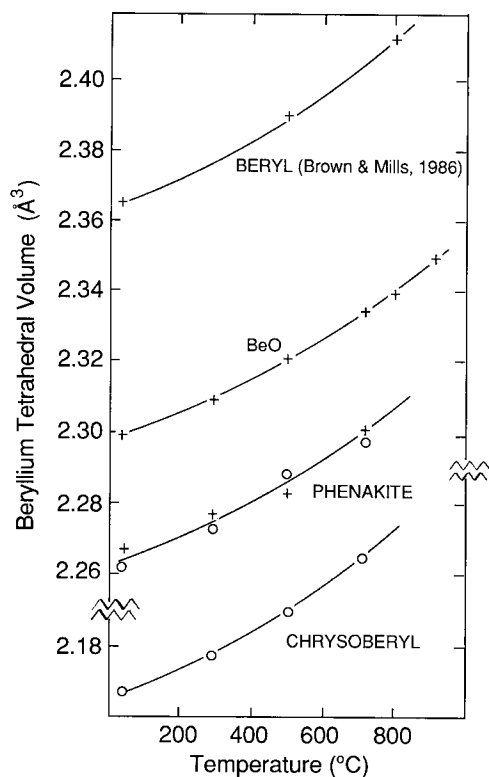


Fig. 3. Polyhedral volume of BeO_4 versus temperature for tetrahedra in phenakite, chrysoberyl, bromellite (Hazen and Finger 1986) and beryl (Brown and Mills 1986)

oxygens all link to one Si and two Be, and in chrysoberyl three Al and one Be coordinate every oxygen. Three different types of oxygens are coordinated to beryllium in beryl: the O2 links to a silicon, an aluminum and a beryllium cation; two O3 oxygens are coordinated to one Si and two Be; and the O5 has an aluminum, a beryllium and a hydrogen as nearest neighbors.

In spite of these differences in size, shape and behavior of the several beryllium tetrahedra, their average volume thermal expansion and its variation with temperature (Fig. 3) are independent of second nearest neighbors. It may be concluded that the shape and asymmetry of the Be—O potential well is similar for all of these structures, even though the position of the minimum (equilibrium Be—O distance) is affected by details of second- and higher-order coordination. This similarity of interatomic potentials from structure to structure is the underlying rationale for the assumption of polyhedral modeling — i.e., that cation coordination polyhedra have properties that are independent of the way in which the polyhedra are linked (Hazen 1987). Other properties of beryllium tetrahedra, including compressibility, fictive heat capacity, and polyhedral elasticity (Au and Hazen 1986; Hazen 1987) also display constant behavior in a variety of beryllium minerals.

High-Temperature Versus High-Pressure Behavior of Beryllium Minerals

Structural changes in phenakite and chrysoberyl at high temperature in many ways mirror those observed at high pressure for these minerals (Hazen and Au 1986; Hazen 1986). Phenakite, for example, varies almost isotropically

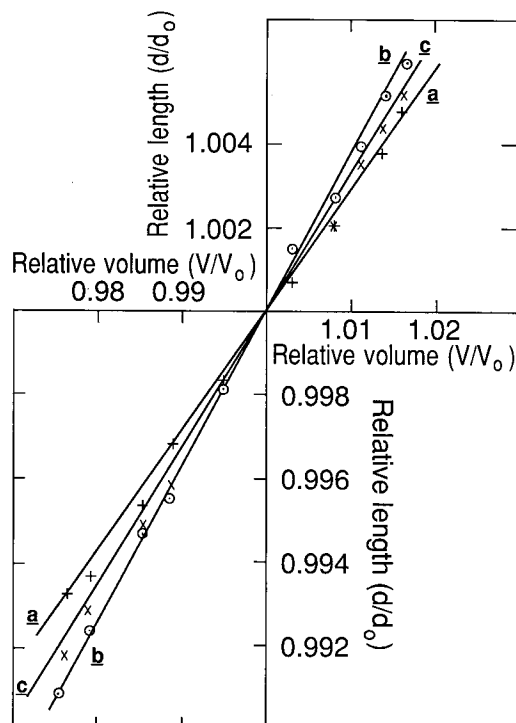


Fig. 4. Relative unit-cell parameters (d/d_0) versus relative unit-cell volume (V/V_0) for chrysoberyl. Circles, points and crosses represent the b , c and a axes, respectively. Points in the upper right represent high-temperature data, whereas those in the lower left represent high-pressure data

with pressure as it does with temperature. The a axis is about 10 percent more compressible than c , whereas the c axis is about 20 percent more expansible than a . In both instances beryllium tetrahedra change volume more than the relatively rigid silicon tetrahedron, and there is no significant distortion of either individual tetrahedra or the tetrahedral framework.

Chrysoberyl displays unusually good correspondence between structural changes on cooling and those on compression. This "inverse relationship" is best illustrated by plots of structural parameters, determined at various temperatures and pressures, versus a normalizing parameter such as relative volume, V/V_0 . Figure 4 illustrates unit-cell parameters of orthorhombic chrysoberyl versus normalized volume. All three unit-cell axes display linear variation versus normalized volume, independent of temperature or pressure. This behavior is typical of most compounds in which all of the constituent polyhedra have similar ratios of polyhedral compression (β between 0 and 50 kbar) to polyhedral expansion (α between 25° and 1000° C). In chrysoberyl both beryllium tetrahedra and aluminum octahedra have polyhedral β/α on the order of 20° C/kbar. This olivine-type mineral, therefore, is expected to display some degree of inverse behavior. In monticellite, the olivine-type $\text{CaMgSi}_2\text{O}_4$, however, β/α for the six-coordinated calcium polyhedron is about 25° C/kbar, whereas that for a magnesium octahedron is about 15° C/kbar. Monticellite, therefore, deviates significantly from the inverse relationship (Sharp et al. 1986).

Acknowledgments. The authors gratefully acknowledge constructive reviews by James W. Downs and Charles T. Prewitt. This

research was supported in part by National Science Foundation Grants EAR83-19209 and EAR84-19982.

References

- Au AY, Hazen RM (1986) Polyhedral modeling of the elastic properties of corundum (α - Al_2O_3) and chrysoberyl ($\text{Al}_2\text{BeSiO}_4$). *Geophys Res Lett* 12:725-728
- Barton MD (1986) Phase equilibria and thermodynamic properties of minerals in the $\text{BeO}-\text{Al}_2\text{O}_3-\text{SiO}_2-\text{H}_2\text{O}$ (BASH) system, with petrologic applications. *Am Mineral* 71:277-300
- Bragg WL, Brown GB (1926) Die Struktur des Olivins. *Z Kristallogr* 63:538-556
- Brown GE Jr, Mills BA (1986) High-temperature structure and crystal chemistry of hydrous alkali-rich beryl from the Harding pegmatite, Taos County, New Mexico. *Am Mineral* 71:547-556
- Downs JW (1983) An experimental examination of the electron distribution in bromellite, BeO , and phenacite, Be_2SiO_4 . Ph.D. Thesis, Virginia Polytechnic Institute and State University, Blacksburg, Virginia
- Farrell EF, Fang JH, Newnham RE (1963) Refinement of the chrysoberyl structure. *Am Mineral* 48:804-810
- Finger LW, Hadidiacos CG, Ohashi Y (1973) A computer-automated, single-crystal, X-ray diffractometer. *Carnegie Inst Washington, Yearb* 72:694-699
- Hamilton WC (1974) Angle settings for four-circle diffractometers. In: *International Tables for x-ray Crystallography* 4:273-284. Kynoch Press, Birmingham, England
- Hazen RM (1985) Comparative crystal chemistry and the polyhedral approach. *Rev Mineral* 14:317-346
- Hazen RM (1986) High-pressure crystal chemistry of chrysoberyl, Al_2BeO_4 : Insights on the origin of olivine elastic anisotropy. *Phys Chem Minerals* 14:13-20
- Hazen RM (1987) A useful fiction: polyhedral modeling of mineral properties. *American Journal of Science*, Wones volume, in review
- Hazen RM, Au AY (1986) High-pressure crystal chemistry of phenakite (Be_2SiO_4) and bertrandite ($\text{Be}_4\text{Si}_2\text{O}_7(\text{OH})_2$). *Phys Chem Minerals* 13:69-78
- Hazen RM, Finger LW (1982) Comparative crystal chemistry. Wiley, New York
- Hazen RM, Finger LW (1986) High-pressure and high-temperature crystal chemistry of beryllium oxide. *J Appl Phys* 59:3728-3733
- Hazen RM, Au AY, Finger LW (1986) High-pressure crystal chemistry of beryl ($\text{Be}_3\text{Al}_2\text{Si}_6\text{O}_{18}$) and euclase ($\text{BeAlSiO}_4\text{OH}$). *Am Mineral* 71:977-984
- Hazen RM, Prewitt CT (1977) Effects of temperature and pressure on interatomic distances in oxides and silicates. *Am Mineral* 62:309-315
- King HE, Finger LW (1979) Diffracted beam crystal centering and its application to high-pressure crystallography. *J Appl Crystallogr* 12:374-378
- Kogure T, Takeuchi Y (1986) Compressibility of the BeO_4 tetrahedra in the crystal structure of phenacite. *Mineral J* 13:22-27
- Morosin B (1972) Structure and thermal expansion of beryl. *Acta Crystallogr B* 28:1899-1903
- Robinson K, Gibbs GV, Ribbe PH (1971) Quadratic elongation: a quantitative measure of distortion in coordination polyhedra. *Science* 172:567-570
- Sharp ZD, Hazen RM, Finger LW (1986) Structural refinements of monticellite to 60 kbar. *Geol Soc Am Abstracts with Progr* 18:746
- Zachariasen WH (1967) A general theory of x-ray diffraction in crystals. *Acta Crystallogr* 23:558-564

Received November 25, 1986